Spectral angular distributions of the X-ray diffraction radiation from an oscillator

1995 J. Phys.: Condens. Matter 7 2909

(http://iopscience.iop.org/0953-8984/7/14/027)

J. Phys.: Condens. Matter 7 (1995) 2909–2915. Printed in the UK

Spectral angular distributions of the x-ray diffraction radiation from an oscillator

O T Gradovsky and A V Ivanova

Institute of Nuclear Problems, Belorussian State University, Bobruiskaya 11, Minsk-50, Belarus

Received 31 August 1994, in final form 30 November 1994

Abstract. The x-ray diffraction radiation from an oscillator (DRO) at a large angle to the particle motion direction is considered. The numerical analysis of the angular and spectral distributions of the x-ray DRO for electrons of medium energies (6–8 MeV) was carried out.

1. Introduction

The influence of the refraction properties of the medium on the radiation spectrum of a moving oscillator was considered by Frank (1942, 1959). As was shown, the frequency ω of the photon emitted at an angle θ relative to the oscillator motion direction is determined by Doppler formulae and is given by

$$\omega = \frac{\Omega}{1 - \beta n \cos\theta} \tag{1}$$

where Ω is the oscillator eigenfrequency, $\beta = v/c$ is the ratio of the speed of oscillator to the speed of light and n is the refractive index. The possibility of a new radiation mechanism conditioned by the complex and anomalous Doppler effects was predicted to arise.

The complex Doppler effect (CDE) occurs owing to the dispersion of the medium when the refractive index is a function of ω. Equation (1) in this case is the equation in ω and there can be several solutions at a fixed angle θ. With the constraint $1 - \beta n \cos\theta < 0$, positive solutions for ω are possible when $\Omega < 0$, i.e. while emitting the oscillator transfers to a higher energy level. This process is called the anomalous Doppler effect (ADE). The case $1 - \beta n \cos\theta = 0$ corresponds to Cerenkov radiation. Apart from characteristic frequencies in an isotropic medium the ADE and Cerenkov radiation manifest themselves only over a soft frequency range (ultraviolet and softer). It is worth noting that all these mechanisms are spatially separated when being observed. In the x-ray range $n = 1 - \omega_L^2/2\omega^2 < 1$ (if the medium is believed to be isotropic) and consequently only the CDE can take place (ω_L is the Langmuir frequency of the medium). As was shown by Baryshevsky and Dubovskaya (1976, 1977) the relativistic electron (positron) channelled in a crystal can serve as an analogue of an oscillator. The eigenfrequency Ω_{if} in this case equals the transition frequency between energy levels (zones) of transverse motion. As follows from the above-mentioned papers the CDE and ADE lead to the conversion of low-frequency oscillations of the particle in a channel to hard x-ray and γ-ray radiation at small angles θ. Thus the study of radiation from channelled (diffracted) particles allows one to investigate the CDE and ADE.

Crystal anisotropy influences not only the motion of a charged particle but also the propagation of radiation itself. In the x-ray range, optical anisotropy is most clearly recognized in the diffraction phenomenon when the refraction properties of the medium change essentially. In this situation the refractive index n depends upon the direction of wave propagation and can exceed unity. On the one hand it may lead (Baryshevsky and Feranchuk 1976) to the generation of parametric x-ray radiation, the analogue of Cerenkov radiation in the x-ray region, which was observed experimentally (Adishev *et al* 1985). On the other hand, when an oscillator moves through the crystal another mechanism of radiation (Baryshevsky and Dubovskaya 1978), which was called the diffraction radiation from an oscillator (DRO) can be initiated. It is physically meaningful that the DRO generation mechanism is not identical with the consecutive addition of the two processes: the radiation from an oscillator and the diffraction of the photons. It was found (Gradovsky 1987) that the spatial distribution of the DRO outside the crystal differs essentially from the diffraction pattern obtained by Laue method when a narrow non-monochromatic x-ray beam is directed towards the static crystal plate. The reason is that the length of the x-ray quantum generated (the coherence length) is much greater than the extinction length of the diffraction and the coherent superposition of radiation and diffraction processes occurs. The spatial distribution of the x-ray DRO for fixed crystallographic planes in the two-beam approximation shows up as two narrow cones: along the motion direction of the oscillator and at a large angle to the motion of direction (figure 1), namely along the vector $\boldsymbol{n}_d = \cos(2\theta_b)\boldsymbol{n}_\parallel + \sin(2\theta_b)\boldsymbol{n}_\perp$ *(figure 1), where* $\theta_b = \sin(|\boldsymbol{\tau}\cdot\boldsymbol{n}_\parallel|/|\boldsymbol{\tau}|)$, $\boldsymbol{n}_\parallel$ *and* $\boldsymbol{n}_\perp$ *are the unit vectors parallel and* perpendicular, respectively, to the motion direction of the oscillator and lie in the diffraction plane and $\boldsymbol{\tau}$ is the reciprocal-lattice vector for given crystallographic planes. In this paper the expressions for the angular distribution of the DRO in the second of the above-mentioned peaks are derived and the numerical calculations for medium-energy electrons channelling in a Si crystal are made.

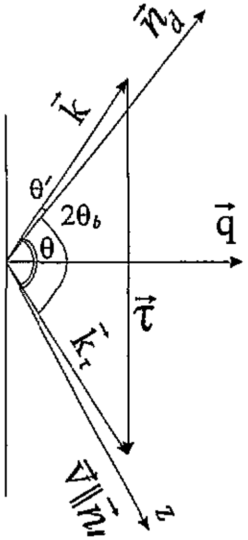

Figure 1. Kinematics of the radiation process in diffraction ($\varphi = 0$).

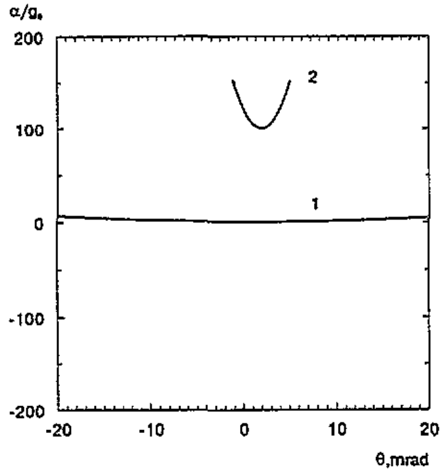

Figure 2. Dependence of α/g_0 upon the radiation angle θ' for electrons having an energy of 6.115 MeV channelled by the (110) planes in silicon and for diffraction by the (202) planes ($d = 1.92$ Å; $\theta_b = 60°$).

2. Dispersion equation for the x-ray diffraction radiation from an oscillator in a side peak

The analysis of energy and momentum conservation laws in a side peak leads to the following frequency angular distribution of the DRO similar to the Doppler formulae:

$$\omega = \frac{\Omega}{1 - \beta n_\tau(\omega, \theta) \cos\theta'} \tag{2}$$

where ω is the radiation frequency, θ is the angle between $\boldsymbol{k}$ (wavevector of the registered wave) and the z axis which is parallel to the particle velocity, θ' is a small angle between $\boldsymbol{k}$ and the vector $\boldsymbol{n}_d$, $n_\tau(\omega, \theta)$ is the refractive index of the diffracted wave having the wavevector $\boldsymbol{k}_\tau$ which is close to the particle motion direction and for the centrally symmetric crystals (Afanasyev and Kagan 1965) given by

$$n_\tau(\omega, \theta) = 1 + \frac{1}{4}\left(\frac{g_0}{\beta_1} + g_0 + \alpha \pm \left\{\left[g_0\left(\frac{1}{\beta_1} - 1\right) + \alpha\right]^2 + 4\frac{g_\tau^2}{\beta_1}\right\}^{1/2}\right) \tag{3}$$

α is the parameter characterizing the deviation from the exact Bragg condition which is given by

$$\begin{gathered} \alpha = \frac{2\boldsymbol{k}(\omega, \theta) \cdot \boldsymbol{\tau} + \tau^2}{k^2(\omega, \theta)} \\ \beta_1 \doteq \frac{\gamma_0}{\gamma_1} \qquad \gamma_0 = \frac{\boldsymbol{k} \cdot \boldsymbol{q}}{|\boldsymbol{k}|} \qquad \gamma_1 = \frac{\boldsymbol{k} \cdot \boldsymbol{q}}{|\boldsymbol{k}_\tau|} \end{gathered} \tag{4}$$

$\boldsymbol{q}$ is the unit vector perpendicular to the crystal surface, g_0 and g_τ are the coefficients defined by the series expansions of the dielectric constant of the crystal versus the reciprocal-lattice vector and the polar angle φ is measured from the x–y plane.

To pass for convenience to the single angle in equation (2) we used the transformation formulae for the rotation of the coordinate system on the $2\theta_b$ angle (Korn and Korn 1961). The refraction index $n_\tau(\omega, \theta)$ may be conveniently written as

$$n_\tau(\omega, \theta) = 1 - \frac{\omega_L^2}{2\omega^2}\Phi(\omega, \theta) \tag{5}$$

where $\Phi(\omega, \theta)$ describes the change in refraction properties of the medium due to the diffraction and it takes the form

$$\Phi(\omega, \theta) = \frac{1}{2}\left[\frac{1}{\beta_1} + 1 - \frac{\alpha}{|g_0|} \mp \sqrt{\left(\frac{1}{\beta_1} - 1 - \frac{\alpha}{|g_0|}\right)^2 + 4\frac{g_\tau^2}{\beta_1 g_0^2}}\right]. \tag{6}$$

In view of equation (5), equation (2) may be rearranged to give

$$\omega = \frac{\Omega}{2(1 - \beta\cos\theta')}\left[1 + \sqrt{1 - 2\left(\frac{\omega_L}{\Omega}\right)^2 \Phi(\omega, \theta)(1 - \beta\cos\theta')\beta\cos\theta'}\right]. \tag{7}$$

So we have the dispersion equation written directly for radiation propagating at a large angle to the oscillator motion direction. Thus we avoid the approximation used frequently in *diffraction considerations when the angle between k and n_d is believed to be approximately* equal to the angle between k_τ and z so that the dispersion equations for radiation propagating in a forward direction and at a large angle are similar. In the general case, equation (7) is the equation of the sixth degree for ω which can be accurately solved only by numerical calculation. This was done in the case of the symmetric diffraction (i.e. $\beta_1 = 1$) for the electrons channelled by the (110) planes in silicon and for diffraction by the (202) planes ($\omega_b = 3.73$ keV). Figures 2 and 3 show such dependences at a fixed angle φ' (0 and π) for the electron energies 6.115 MeV and 6.13 MeV, respectively. The dispersion curves 1 and 2 are the solutions of equation (4) and are continuous within the whole angular range unlike the dispersion curves for the radiation propagating in a forward direction when there is an angular interval 10^{-5}–10^{-4} rad within which the generation of x-rays is forbidden (Gradovsky 1987, Gradovsky and Ivanova 1994). At the energies in question the maximum radiation frequency of the channelled electrons can be less or greater than the Bragg frequency for a given direction ($\omega_{\max} = 2\gamma^2\Omega$ when $\theta' = 0$) that reflects the character of the dispersion curves of the x-ray DRO. When $\omega_{\max} < \omega_b$ (figure 2), the dispersion curves have the break in α. When $\omega_{\max} \geqslant \omega_b$ (figure 3) the dispersion curves intersect the line $\alpha/g_0 = 0$. The general view of the spectral distributions are similar to figures 2 and 3, but the behaviour of the dispersion curves is clearer when observing the dependence of α/g_0 upon the angle θ'.

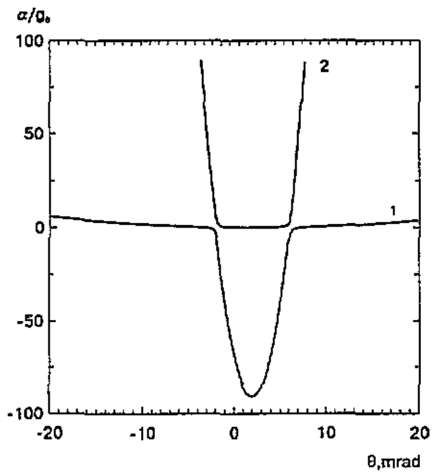

Figure 3. As for figure 2 but for electrons having an energy of 6.13 MeV.

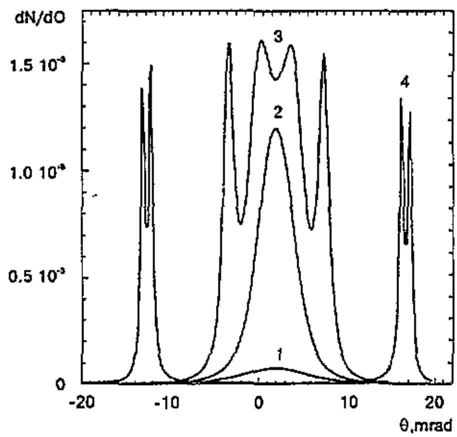

Figure 4. The angular distributions of the x-ray diffraction radiation from electrons at energies of 6.1 MeV (curve 1), 6.115 MeV (curve 2), 6.13 MeV (curve 3) and 6.22 MeV (curve 4).

It should be stressed here that the spectral and angular ranges of the x-ray DRO far exceed (by an order of magnitude or more than) the regular half-widths of the appropriate diffraction peaks. The variation in the x-ray DRO frequencies with the change in radiation angle described by equation (7) is of particular interest when preparing the two-crystal scheme of the experiment for studying the fine structure of the DRO peaks.

3. Spectral angular distribution of the x-ray diffraction radiation from an oscillator in a side peak

The spectral angular distribution of the x-ray DRO at a large angle within the limits of the dipole and two-beam approximations ($\omega \ll E$) has the form ($\hbar = c = 1$) (Baryshevsky and Dubovskaya 1978, 1983)

$$\frac{\mathrm{d}^2 N_s}{\mathrm{d}\omega\,\mathrm{d}\Omega} = \frac{e^2\omega}{2\pi}\sum_{nf} Q_{nn}|e_{1s}\cdot g_{nf}|^2|X_{nf}|^2|\xi^{\tau}_{\mu s}|^2\left|\frac{\sin(q^{\mu s}_{znf}L)}{q^{\mu s}_{znf}}\right|^2 \tag{8}$$

where $\xi^{\tau}_{\mu s} = \mp g_{\tau s}/2(\varepsilon_{2s} - \varepsilon_{1s})$ (s $= \sigma, \pi$ correspond to the σ and π polarizations of the photon; $\mu = 1, 2$ specify two dispersion branches; $g_{\tau s} = C_s g_\tau$; $C_\sigma = 1$; $C_\pi = \cos(2\theta_b)$; the negative sign relates to $\mu = 1$ and the positive to $\mu = 2$),

$$\varepsilon_{\mu s} = \tfrac{1}{4}\{g_0 + \beta_1 g_0 - \beta_1\alpha \pm [(g_0 + \beta_1 g_0 - \beta_1\alpha)^2 + 4\beta_1(\alpha g_0 - g_0^2 + g_{\tau s}^2)]^{1/2}\} \tag{9}$$

L is the crystal length, Q_{nn} is the probability that the transverse energy state n is populated, e_{1s} are the vectors defining the photon polarization $g_{nf} = \Omega_{nf}\boldsymbol{n}_{\parallel} + \beta k_{\tau x}\boldsymbol{n}_{\perp}$ (in the case of plane channelling) where n and f are the numbers of the particle transverse energy zones, X_{nf} is the coordinate matrix transition coefficient, $(q^{\mu s}_{znf})^{-1}$ is the coherent length which is given by $(q^{\mu s}_{znf})^{-1} = p_{zi} - p_{1zf} - k_{\tau z} - \omega\varepsilon_{\mu s}/\gamma_1$, where p_{zi} and p_{1zf} are the longitudinal components of the particle momentum.

Having integrated over ω (with due account of the relationship $[\sin^2(q^{\mu s}_{znf}L)]/q^{\mu s}_{znf} \simeq 2\pi L\delta(q^{\mu s}_{znf})$ for sufficiently thick crystals) the expression for angular distribution of the DRO in the side diffraction maximum was obtained:

$$\frac{\mathrm{d}N}{\mathrm{d}O} = \sum_{nfs}\frac{Le^2\omega Q_{nn}|\xi^{\tau}_{\mu s}|^2|X_{nf}|^2[f_1(\theta) + f_2(\theta)]}{2\pi|\Omega/\omega - \beta\cos\theta'\{(\omega_{\mathrm{L}}/\omega)^2\Phi(\omega,\theta) - (\omega_{\mathrm{L}}^2/2\omega)[\partial\Phi(\omega,\theta)/\partial\omega]\}|} \tag{10}$$

where

$$f_1(\theta) = \frac{k_{\tau y}^2(\Omega\sin\theta_b + \beta c k_{\tau x}\cos\theta_b)^2}{k^2 - (k\sin\theta - k\cos\theta)^2}$$

$$f_2(\theta) = \frac{\{\Omega[\cos\theta_b(k_{\tau z}^2 + k_{\tau y}^2) + k_{\tau z}k_{\tau x}\sin\theta_b] + k_{\tau z}k_{\tau x}\sin\theta_b\}^2}{k_\tau^2(k_\tau^2 - k_{\tau z}\sin\theta_b - k_{\tau x}\cos\theta_b)^2} - \frac{\beta c k_{\tau x}[k_{\tau x}k_{\tau z}\cos\theta_b + (k_{\tau y}^2 + k_{\tau x}^2)\sin\theta_b]}{k_\tau^2[k_\tau^2 - (k_{\tau z}\sin\theta_b - k_{\tau x}\cos\theta_b)^2]}$$

$$k_{\tau x} = k\sin\theta\cos\varphi - \tau\cos\theta_b$$

$$k_{\tau y} = k\sin\varphi\sin\theta$$

$$k_{\tau z} = k\cos\theta - \tau\sin\theta_b$$

$$k_\tau = k_0\left(n + \frac{\alpha}{2}\right)$$

and k_0 is the wavevector in vacuum.

The angular distributions of the x-ray DRO calculated according to (10) for the two-level system under the above-mentioned conditions with electron energies of 6.1 MeV (curve 1), 6.115 MeV (curve 2), 6.13 MeV (curve 3) and 6.22 MeV (curve 4) are given in figure 4. For curves 1 and 2, only one of the dispersion branches contributes to the angular distribution when $\alpha \simeq g_0$ (figure 2, curve 1). Curve 3 corresponds to the case $\omega_{\max} \approx \omega_b$ and the second dispersion curve is initiated (figure 3, curve 2). Peaks appropriate to the different dispersion branches vary in angular position, which leads to the fine structure of the x-ray DRO peaks (figure 4, curves 3 and 4). With further energy increase the peaks shrink and, at the energy of 6.22 MeV, $\Delta\theta'$ equals 2×10^{-3} rad. Let us note that the x-ray DRO has a threshold character; near some value of the electron energy the DRO intensity rises sharply by a factor of almost 20 under a slight energy variation by 0.3% (curves 1 and 2). To follow the further dynamics of the x-ray DRO the dependence of the peak of angular distribution upon the electron energy is presented in figure 5 (curve 1 for $\varphi = 0$ and curve 2 for $\varphi = \pi/2$). After a sharp increase at the energy of 6.13 MeV the peak intensity smoothly falls for $\varphi = \pi/2$ and has an extremum at an energy of 10 MeV for $\varphi = 0$.

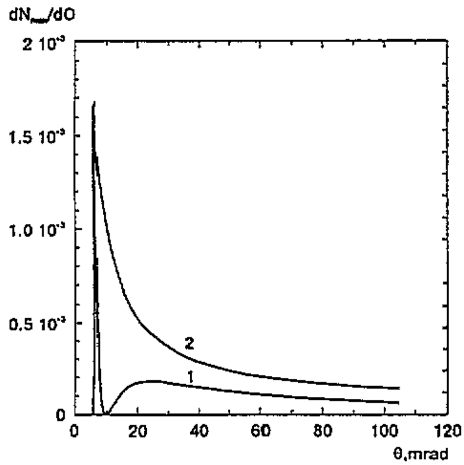

Figure 5. Dependence of the peak intensity of angular distribution upon the electron energy for $\varphi = 0$ (curve 1) and $\varphi = \pi/2$ (curve 2).

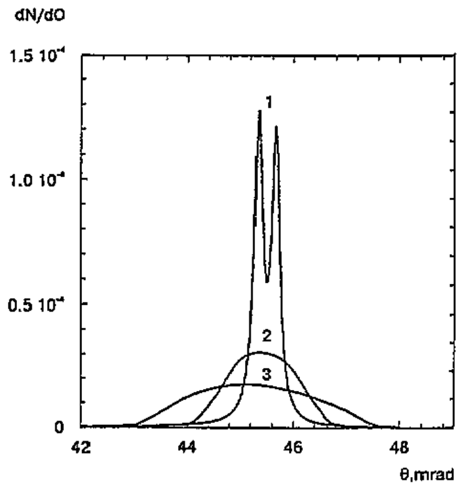

Figure 6. Angular distribution of the x-ray DRO at an average energy of the electrons of 8 MeV and with electron beam spreads $\Delta E/E$ of 1% (curve 2) and 2% (curve 3). The angular distribution of the DRO for single-energy electrons having an energy of 8 MeV is also shown (curve 1).

Therefore, like the radiation propagating in a forward direction the DRO at a large angle to the motion direction bears a threshold character and strongly depends on the oscillator energy. That is why, in order to evaluate the width and the intensity of the peaks for the experimental observation, it is necessary to take into account a spread of energies in the electron beam. The x-ray DRO angular distributions for the electron beam at an average energy of 8 MeV with spreads of 1% (figure 6, curve 2) and 2% (figure 6, curve 3) have been calculated. One can see that the peak intensity falls by a factor of approximately 4 at a 1% beam spread and by a factor of 8 at 2% while the peak widths rise by the same factors, correspondingly. It should be noted that the influence of the spread in energies on the angular distribution of the x-ray DRO propagating in a forward direction is greater than on that propagating at a large angle to the motion direction (Gradovsky and Ivanova 1994) so that for the single-energy beams the side peak is much wider (e.g. at an energy of 8 MeV the half-width of the side peak is greater by a factor of 5 than that of the forward peak) while in view of the energy spread the half-widths of the side and forward peaks are the same.

The x-ray DRO yield of the electron beam having an average current $I = 10$ nA at the energy of 8 MeV within the angular range $\Delta\Omega \simeq 10^{-3}$ rad comprises 5×10^4 quanta s^{-1} which allows one to investigate the DRO by common scanning of the angular distributions.

4. Conclusion

Thus the differences obtained between the x-ray DRO characteristics for the radiation in the forward and in the side diffraction maximum indicate the necessity of solving the dispersion equation written directly for the radiation propagating at a large angle to the oscillator motion direction.

References

Adishev Yu N, Baryshevsky V G, Vorobev S A, Danilov V A, Pak S D, Potylitsin A P, Safronov P F, Feranchuk I D and Sherepitsa S V 1985 *Zh. Exp. Teor. Fiz. Pis. Red.* **74** 295

Afanasyev A and Kagan Yu 1965 *Zh. Exp. Teor. Fiz.* **48** 327

Baryshevsky V G and Dubovskaya I Ya 1976 *Dokl. Akad. Nauk SSSR* **231** 1335

—— 1977 *Phys. Status Solidi* b **82** 403

—— 1978 *Phys. Status Solidi* b **88** 351

—— 1983 *J. Phys. C: Solid State Phys.* **16** 13663

Baryshevsky V G and Feranchuk I D 1976 *Phys. Lett.* **57A** 183

Frank I M 1942 *Izv. Akad. Nauk SSSR, Ser. Fiz.* **6** 3

—— 1959 *Pis. Zh. Eksp. Teor. Fiz.* **36** 823

Gradovsky O T 1987 *Phys. Lett.* **126A** 291

Gradovsky O T and Ivanova A V 1994 *Vesci Akad. Nauk, Ser. Fiz.-Mater.* **2** 83

Korn G A and Korn T M 1961 *Mathematical Handbook for Scientists and Engineers* (New York: McGraw-Hill)